Abrupt Climate Change Triggered by GIN Sea Convection

Abstract

In the IPCC report, the warming at the end of 21st century is projected as between two and four degree Celsius. But this is the statement based on the equilibrium sensitivity, and the climate system is bound to exhibit wild swaying of the abrupt climate change through the transient and nonlinear dynamics, especially in the polar region. In order to provide more accurate projection in the future, it is necessary to demonstrate that the IPCC-type models have the capability to simulate abrupt climate change, for example, the Bølling-Allerød (BA) warming trend that began 15,000 years ago and eventually ended the last ice age.

We conducted the first synchronously coupled atmosphere-ocean general circulation model simulation of the transient evolution of global climate from the Last Glacial Maximum 21,000 years ago to the abrupt BA warming 14,500 years ago. Our model reproduces the major features of the evolution of deglacial climate change, including the magnitude of the climate response, suggesting good agreement between observed and model climate sensitivity. The model simulates the BA warming as a transient response of the Atlantic meridional overturning circulation (AMOC) to the termination of imposed freshwater discharge associated with Heinrich event 1 (H1).

In the ramped forcing scenario, the freshwater forcing is slowing down gradually in the north Atlantic ocean, but an abrupt warming event occurs before the freshwater forcing zeros out: in four decades, the surface air temperature in GIN Sea shoots up from -10 ^{o}C to above freezing. This abrupt warming is triggered by the sudden switch–on of the GIN convection and the rapid opening the sea ice in the GIN sea. The ocean subsurface warming after H1 and the surface evaporation after the sea ice opening appear to be important processes that generate positive salinity anomaly in the GIN Sea and switch the Atlantic meridional overturning circulation from the glacial cold mode to the present-day warm mode.

Introduction

One of the most striking features of the last deglaciation is the millennial climatic events that punctuated the overall warming trend from the Greenland ice core. The connections between the ice cores and ocean sediment have been suggested to be caused by the variability of AMOC [Broecker, 1998]. Recent reconstruction of AMOC via Pa/Th [McManus et al., 2004] provides further evidence that the variability of AMOC plays a critical role in modulating the millennial climate events during the whole period of the deglaciation. Furthermore, on decadal time scale, abrupt climate change has also been suggested to have occurred due to the sudden changes of AMOC. [Lehman and Keigwin, 1992] documented abrupt change of Sea Surface Temperature (SST) and Surface Air Temperature (SAT) in the North Atlantic region caused by the flow of the Atlantic warm water into the GIN seas.

In order to better predict the climate change in the future, it is urgent to demonstrate that the IPCC-type climate models not only have the correct climate

sensitivity to green house gas, but also could simulate the abrupt climate change due to sudden changes of AMOC and/or sea ice.

Model and experiment design

The close relationship between AMOC and ice core record enables us to use the AMOC as the benchmark for the simulation of the last deglaciation. AMOC has been shown to be quite sensitive to the surface freshwater fluxes [Rahmstorf, 1995] and could have the hysteresis behavior in simple box models [Stommel, 1961] and more complex ocean general circulation models [Rahmstorf et al., 2005]. Both high sensitivity and the hysteresis of AMOC to the melting water forcing (MWF) provide the possibilities of simulating the abrupt climate change at the onset of BA warming.

After the collapsed of AMOC at 17.0ka BP, two schemes of MWF were employed to test the sensitivity of climate system to the rate of the reduction of the MWF. In scheme DGL-A (Fig. 1c), MWF in Gulf of Mexico was shut off immediately after 17.0ka, while MWF in North Atlantic remained at 15 m/kyr until it was suddenly shut off at 14.67ka. In scheme DGL-B (Fig. 2c), MWF linearly decreased from 20 m/kyr to 0 between 17.0ka and 14.2 ka.

The simulation of the onset of BA warming

For DGL-A, after we shut off the hosing at 14.7ka, the rebound of AMOC closely follows the AMOC reconstruction with 5~6 Sv (1Sv = 10^6 m^3/s) overshoot in the end of the BA warming (Fig. 1a). Given the fact that the time scale of the rebound is solely determined by the model in DGL-A, we demonstrate the abrupt increase of AMOC from

Pa/Th reconstruction could be simulated via the maximum recovery rate of AMOC in CCSM3. At Greenland, the increase of SAT due to the abrupt resumption of AMOC matches the temperature reconstruction from GISP2 ice core record in terms of both recovery rate and the amplitude (Fig. 1b). In summary, CCSM3 could simulate the onset of BA warming as the transient response to the abrupt resumption of AMOC after its collapse during H1.

In DGL-B, AMOC starts to increase as MWF decreases gradually toward BA. Even though the reduction of MWF is linear (Fig. 2c), the response of AMOC to the ramped forcing exhibit nonlinearity (Fig. 2a). AMOC starts to increase slowly to 5 Sv as MWF drops from 20m/kyr to 10m/kyr, then AMOC increases more quickly to 10Sv when MWF drops from 10m/kyr to 5 m/kyr. Then the increase of AMOC becomes slower when MWF drops from 5m/kyr to 2 m/kyr before the abrupt increase of AMOC from 12Sv to 17Sv in less than 2m/kyr change of MWF. The modeled GISP2 temperature closely follows the change of AMOC and exhibits a similar nonlinear variability under the linear reduction of MWF. Compared to DGL-A, even though DGL-B fails to simulate the abrupt resumption of AMOC as reconstructed from Pa/Th, both AMOC and modeled GISP2 temperature reach the similar amplitude: from H1 to the onset of BA, AMOC increases from 3Sv to 17Sv and GISP2 temperature increases from -45C to -29C.

The 5~6 Sv overshoot of AMOC is pivotal for the successful simulation of the amplitude of BA warming in both MWF schemes. The mechanism of the overshoot is hard to be investigated in DGL-A due to its transient behavior. However, there should be more clues of the mechanism of the overshoot from DGL-B, as the model undergoes quasi-equilibrium through the slow change of the ramped forcing. In fact, it is readily to

see that the abrupt increase of AMOC near the end of ramped MWF forcing produced the overshoot of AMOC in DGL-B.

Abrupt climate change in DGL-B

Abrupt climate change could be defined as a large-scale change that happens more quickly than that brought on by forcing mechanisms – on a scale of years to decades, not centuries – and that persists for a very long time. This statement emphasizes the importance of the nonlinearity in the abrupt climate change ---- the climate should change more quickly than the external forcing. In the scheme of DGL-A, the climate response is as quick as the MWF forcing, so abrupt change of AMOC and modeled GISP2 temperature could not be regarded as abrupt climate change. However, near the end of DGL-B, the change of AMOC and GISP2 temperature is much quicker than the linear reduction of MWF and should be regarded as one example of abrupt climate change. In this scenario, since the forcing is linearly reduced and gives no clue on the timing of the abrupt change, the climate system must have passed certain threshold before abrupt climate change occurs. Therefore, the search for the specific threshold is key to the abrupt climate change study.

GIN sea convection as the trigger for abrupt climate change

We use figure 3 to illustrate that GIN convection provides the threshold mechanism for the abrupt climate change that produces the overshoot of AMOC. In just four decades of the end of the DGL-B, the surface air temperature in GIN sea shoots up from -10 ^{o}C to above freezing and it still increases afterward with a slower rate (Fig.3a).

This abrupt warming is happening in the whole GIN Sea (Fig. 3b) and even contributes to the rapid warming in Greenland (Fig. 3a, blue). The sea ice concentration in this region also reduces from 60% to 10%. This abrupt warming is triggered by the sudden switch–on of the GIN convection (Fig. 3c) as inferred from the maximum mix layer depth, which remains around 50m for 7500 years since 22ka before the sudden change to 350 m in less than four decades.

After the sea ice opening, massive heat fluxes (Fig. 4) with maximum value around 100 W/m2 is transferred from the ocean into the atmosphere to account for the sudden atmosphere temperature increase. These heat fluxes are mainly from the sensible and latent heat fluxes (Fig. 5) , consistent with situation of the sea ice opening. The upward heat fluxes excludes any scenarios that the atmosphere triggers the abrupt climate change.

At ocean surface (Fig. 6), the sea surface temperature (SST) increases by 3~5 degrees. The increase of SST in spite of the upward heat flux implies the vertical and horizontal heat transports provide the heat flux that warms the GIN sea. Sea surface salinity (SSS) also increases by 1 psu. The increase of SSS partly results from the increase of net evaporation (Fig. 7). In the polar region, the potential density (PD) is strongly influences by SSS. Therefore, the increase of SSS results in the increase of PD that induces the abrupt increase of AMOC.

From the zonal mean Atlantic section (Fig. 8), AMOC increases by more than 3 Sv on the latitude of 60N, consistent with the latitude of the increase of PD and SSS. The maximum change of PD and SST are at the surface, strongly suggesting that the evaporation increase after the sea ice opening plays dominant role on the abrupt change

of SSS/PD and AMOC.

The penetration of the warm water from North Atlantic into GIN sea is readily seen from the change of ocean current at 100m (Fig. 9a). An anti-clockwise circulation forms in the GIN sea with the maximum change of ocean current as high as 5 cm/s. This is almost as large as the climatological value (Fig. 9b), which means 100% increase of ocean current in the GIN sea.

Conclusion

The abrupt climate change at the end of the ramped forcing scenario is triggered by the convection in GIN Sea, which haven't formed deep water for 7500 years since 22ka before the deep water formation suddenly occurs in less than four decades during the onset of BA warming. The convection in GIN sea quickly induces sea ice opening after the warm water from subsurface ocean rises to the surface. After sea ice opening, evaporation induces surface salinity increases that induces the increases of surface density. The increase of surface density induces the abrupt increase of AMOC and more heat transport and more sea ice opening. The formed positive feedback quickly increases GIN sea surface temperature from -10 to above freezing in less than 4 decades. What triggers the start of convection in GIN sea needs further investigation.

Reference

Broecker, W. S., 1998: Paleocean circulation during the last deglaciation: A bipolar seesaw. *Paleoceanography,* **13**, 119-121.

Lehman, S. J. and L.D. Keigwin (1992). Sudden changes in the North Atlantic circulation during the last deglaciation. Nature 356: 757-762.

McManus, J. F., R. Francois, J. -. Gherardi, L. D. Keigwin, and S. Brown-Leger, 2004: Collapse and rapid resumption of Atlantic meridional circulation linked to deglacial climate changes. *Nature*, **428**, 834-837.

Rahmstorf, S., 1995: Bifurcations of the Atlantic thermohaline circulation in response to changes in the hydrological cycle. *Nature*, **378**, 145-149.

Rahmstorf, S., M. Crucifix, A. Ganopolski, H. Goosse, I. Kamenkovich, R. Knutti, G. Lohmann, R. Marsh, L. A. Mysak, and Z. Wang, 2005: Thermohaline circulation hysteresis: A model intercomparison. *Geophys.Res.Lett.*, **32**, L23605.

Stommel, H., 1961: Thermohaline convection with two stable regimes of flow. *Tellus*, **13**, 224-230.

Figure Caption

Fig.1. Simulations (blue) and reconstructions (red) of AMOC (upper left), GISP2 SAT (upper right) and the associated melting water forcing (lower left) and sea level rise (lower right) for DGL-A. The hosing is stopped at 14.7ka. The sea level rise reconstruction is from Peltier 2004.

Fig. 2. Same as Fig. 1, but for DGL-B. After H1, the hosing rate is reduced from 20m/kyr to 0m/kyr between 17.0ka and 14.2ka.

Fig. 3. The abrupt climate change Triggered by GIN Sea Convection. Upper right: GIN Sea SAT time series (black) and Greenland SAT time series (blue). The 40-year abrupt climate change is highlighted in red. Upper left, SAT difference after the 40-year abrupt

climate change. Lower left, same as the plot of upper right, but for maximum convective depth in GIN Sea. Lower right, same as the plot of upper right, but for sea ice reduction in GIN Sea.

Fig. 4. Total surface heat flux difference after the 40-year abrupt climate change

Fig. 5. Sensible (SHFLX), latent (LHFLX), net shortwave (FSNS) and net longwave (FLNS) heat flux difference after the 40-year abrupt climate change

Fig. 6. Sea surface temperature (SST), sea surface salinity (SSS), potential density (PD) difference after the 40-year abrupt climate change

Fig. 7. Precipitation minus evaporation (P-E), Precipitation (PRECIP), evaporation (EVAP) difference after the 40-year abrupt climate change

Fig. 8. The difference of Atlantic zonal average of AMOC, salinity and potential density after the 40-year abrupt climate change

Fig. 9. (Upper) the difference of 100m ocean current after the 40-year abrupt climate change. (Lower) the climatology of 100m ocean current at LGM

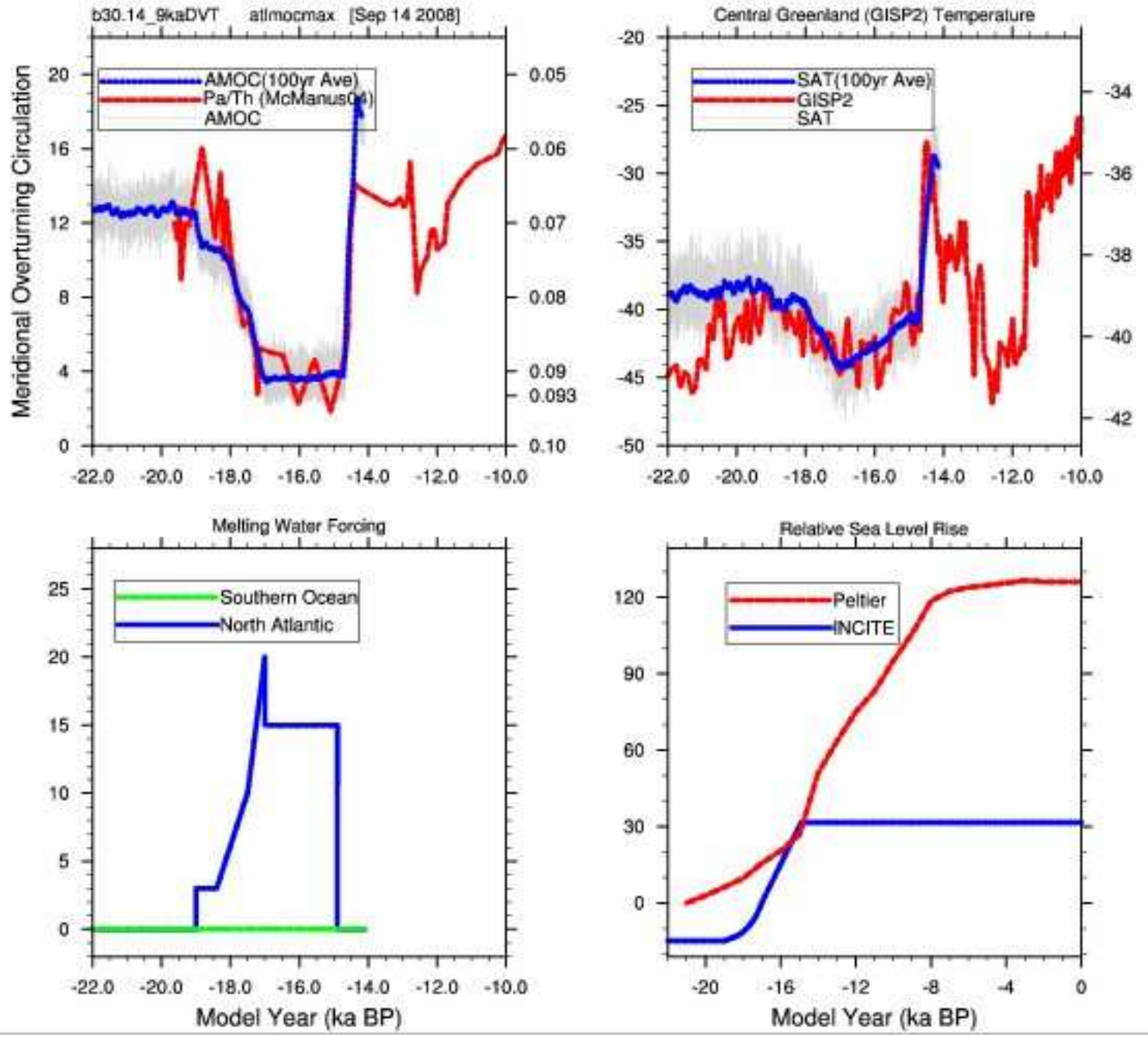
b30.14_9kaDVT atlmocmax [Sep 14 2008]
Meridional Overturning Circulation
AMOC(100yr Ave)
Pa/Th (McManus04)
AMOC
Central Greenland (GISP2) Temperature
SAT(100yr Ave)
GISP2
SAT
Melting Water Forcing
Southern Ocean
North Atlantic
Relative Sea Level Rise
Peltier
INCITE
Model Year (ka BP)
Model Year (ka BP)

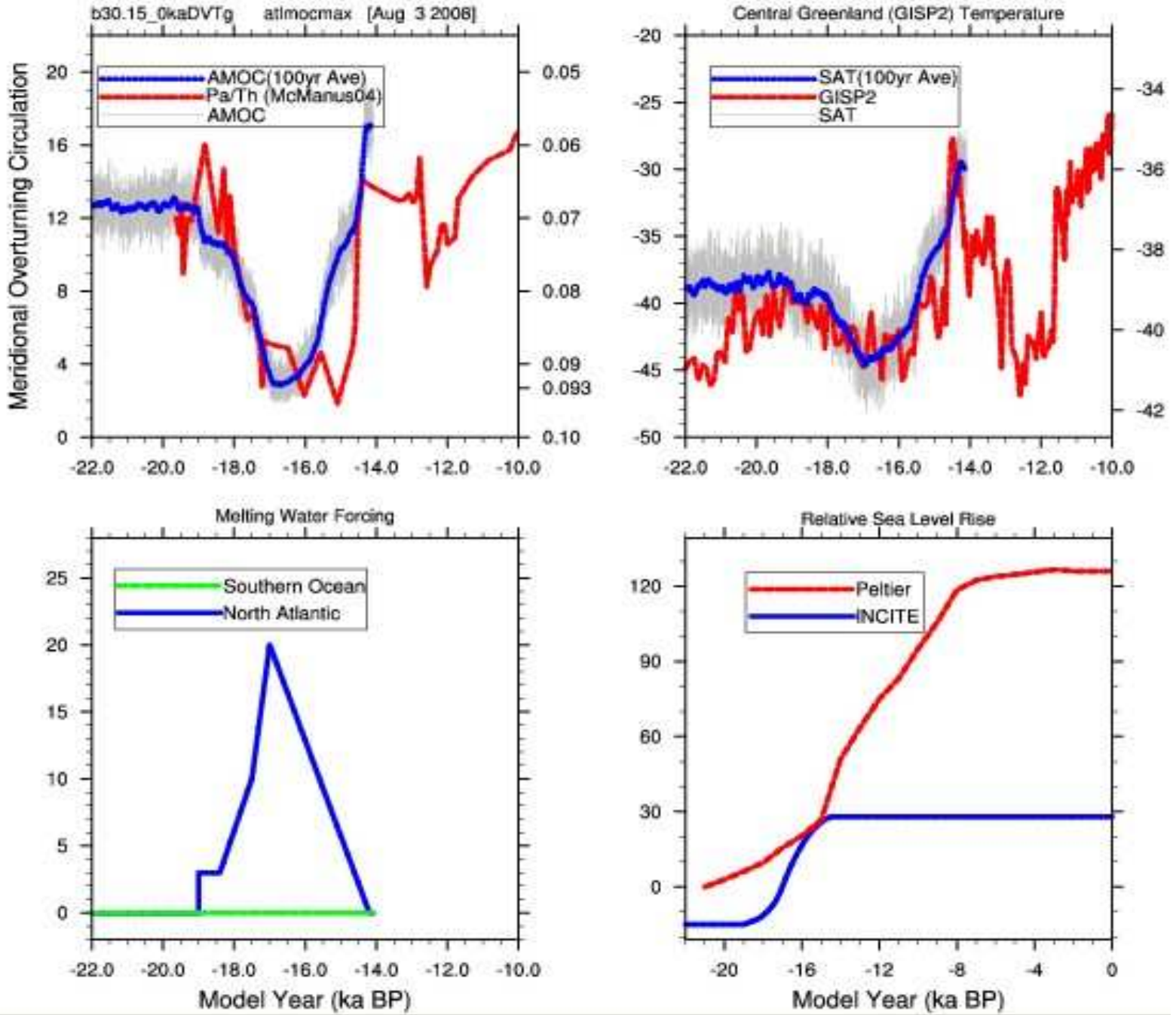
b30.15_0kaDVTg atlmocmax [Aug 3 2008]
Meridional Overturning Circulation
AMOC(100yr Ave)
Pa/Th (McManus04)
AMOC
Central Greenland (GISP2) Temperature
SAT(100yr Ave)
GISP2
SAT
Melting Water Forcing
Southern Ocean
North Atlantic
Model Year (ka BP)
Relative Sea Level Rise
Peltier
INCITE
Model Year (ka BP)

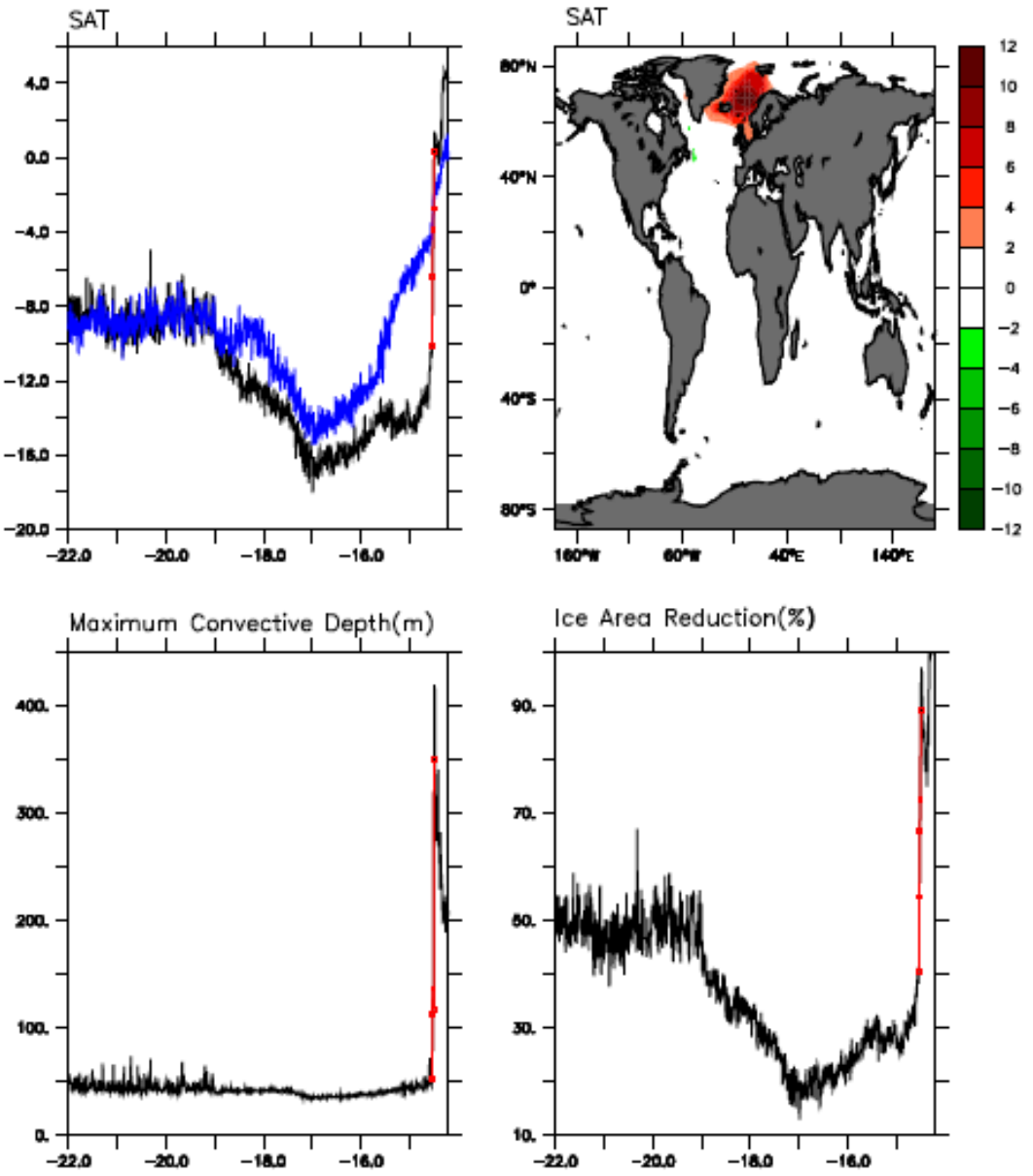
SAT
4.0
0.0
-4.0
-8.0
-12.0
-16.0
-20.0
-22.0
-20.0
-18.0
-16.0
SAT
80°N
40°N
0°
40°S
80°S
160°W
80°W
40°E
140°E
12
10
8
6
4
2
0
-2
-4
-6
-8
-10
-12
Maximum Convective Depth(m)
400.
300.
200.
100.
0.
-22.0
-20.0
-18.0
-16.0
Ice Area Reduction(%)
90.
70.
50.
30.
10.
-22.0
-20.0
-18.0
-16.0

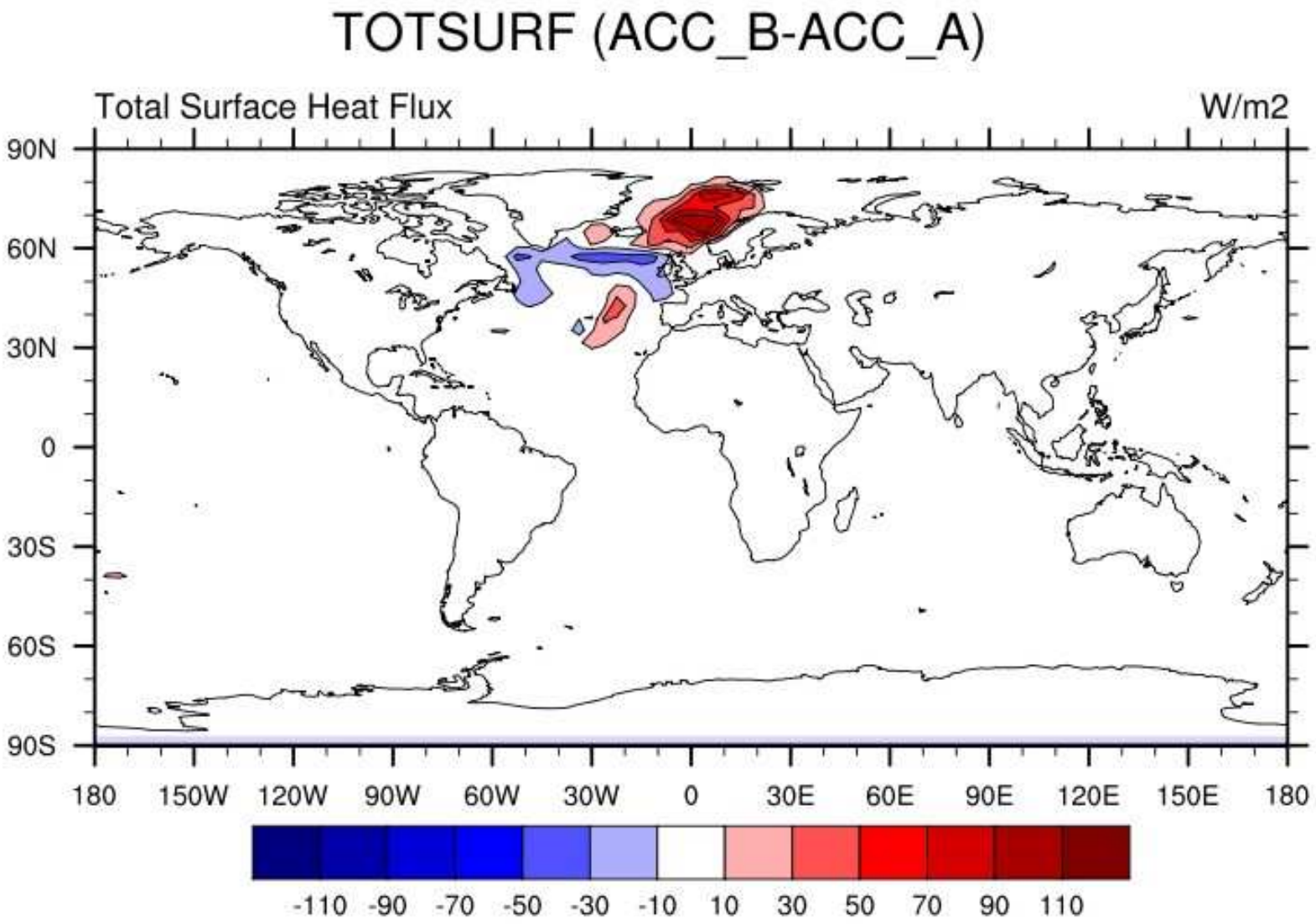
TOTSURF (ACC_B-ACC_A)
Total Surface Heat Flux
W/m2
90N
60N
30N
0
30S
60S
90S
180
150W
120W
90W
60W
30W
0
30E
60E
90E
120E
150E
180
-110
-90
-70
-50
-30
-10
10
30
50
70
90
110

SHFLX (ACC_B-ACC_A)

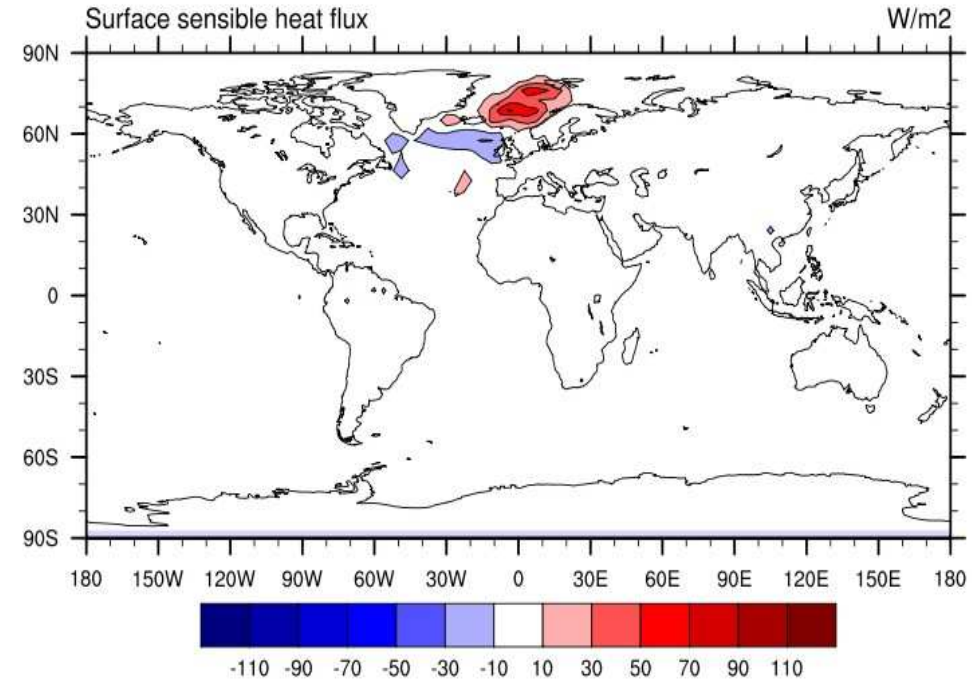

FSNS (ACC_B-ACC_A)

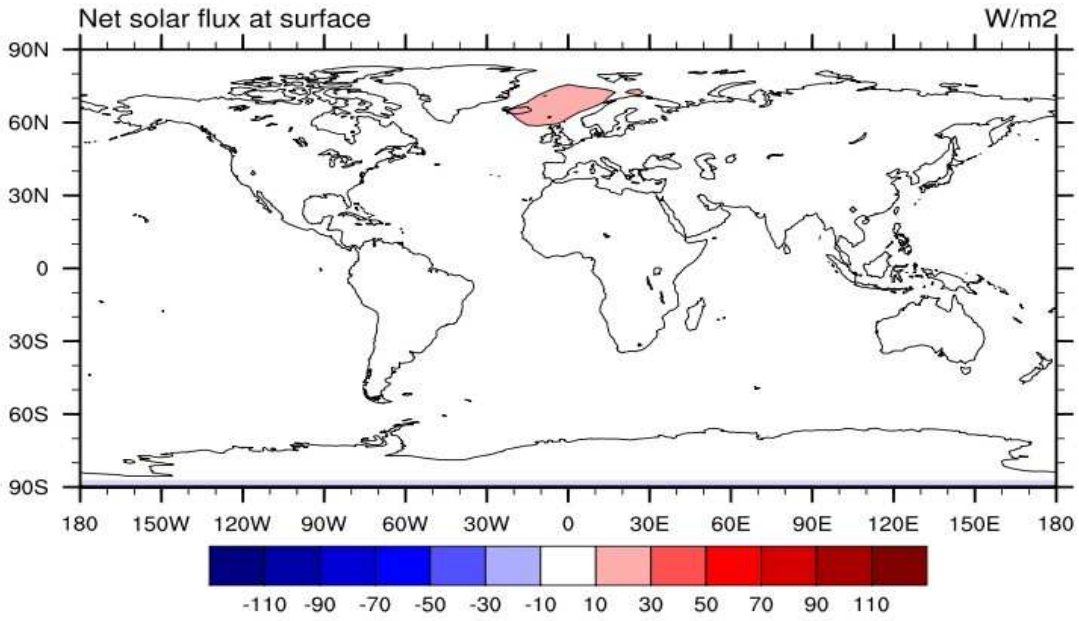

LHFLX (ACC_B-ACC_A)

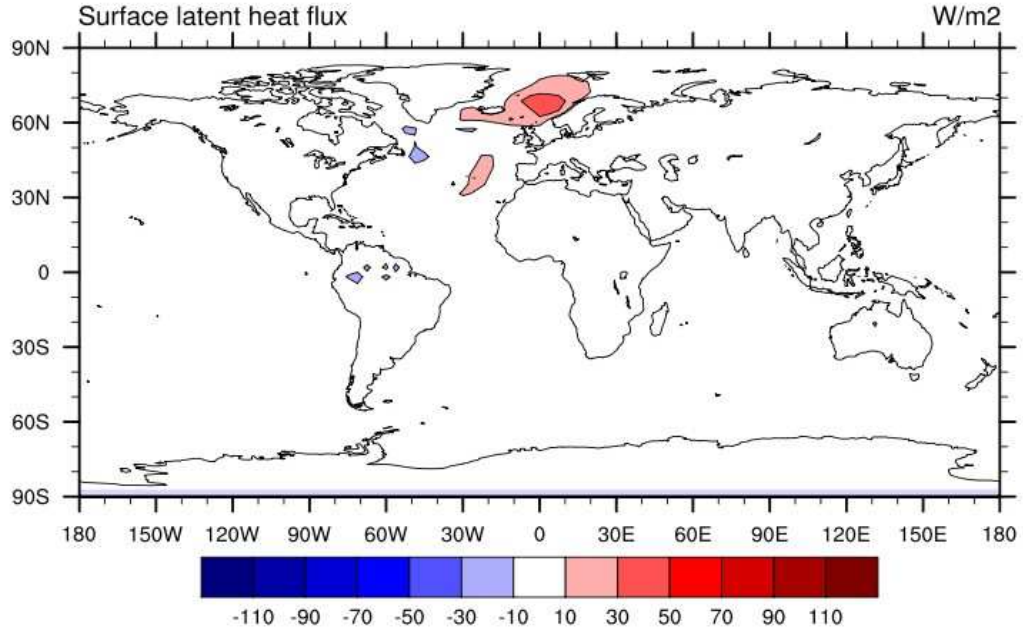

FLNS (ACC_B-ACC_A)

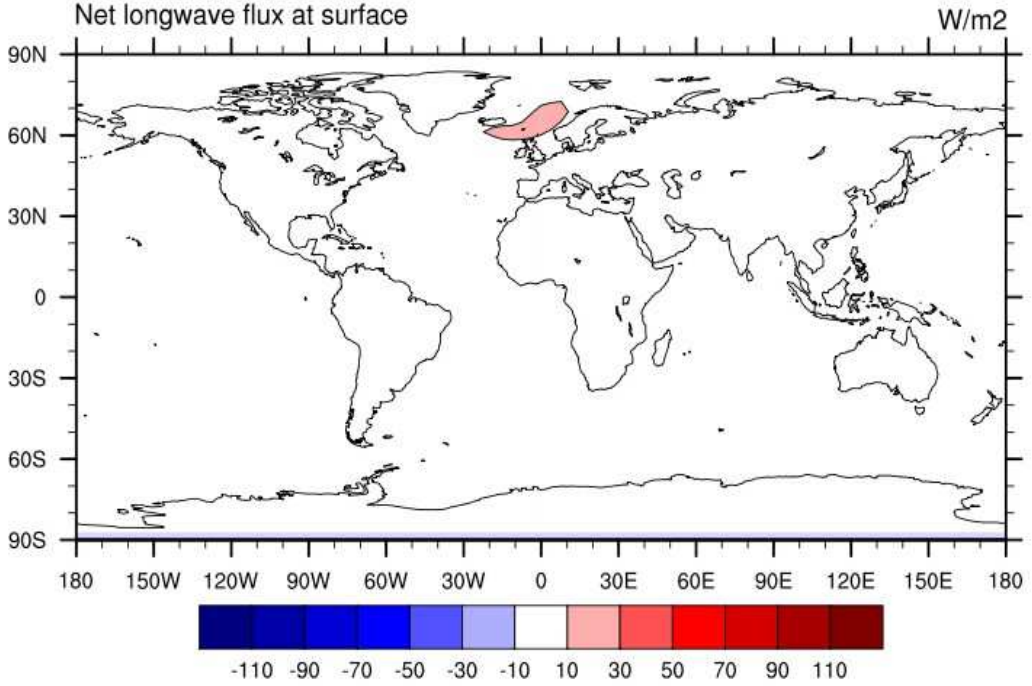

SST (ACC_B-ACC_A)

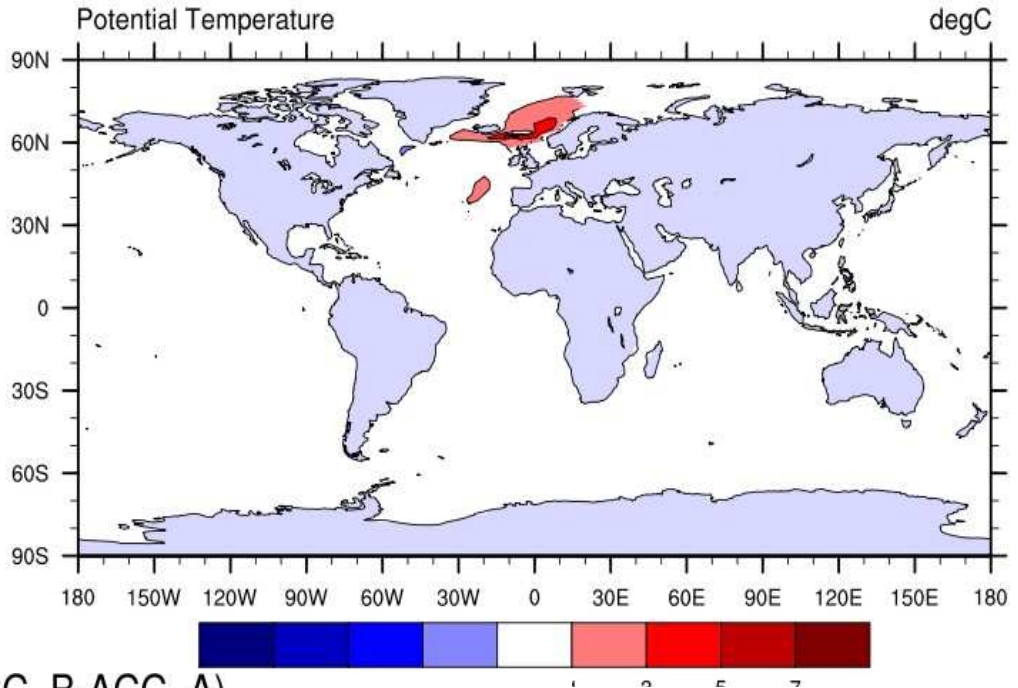

SSS (ACC_B-ACC_A)

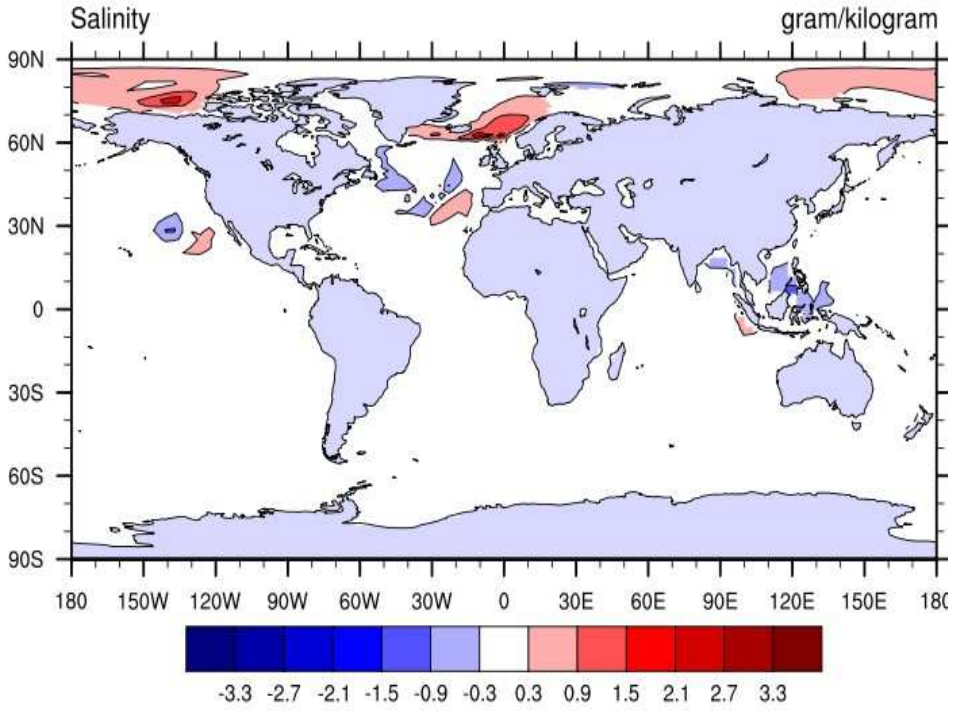

PD (ACC_B-ACC_A)

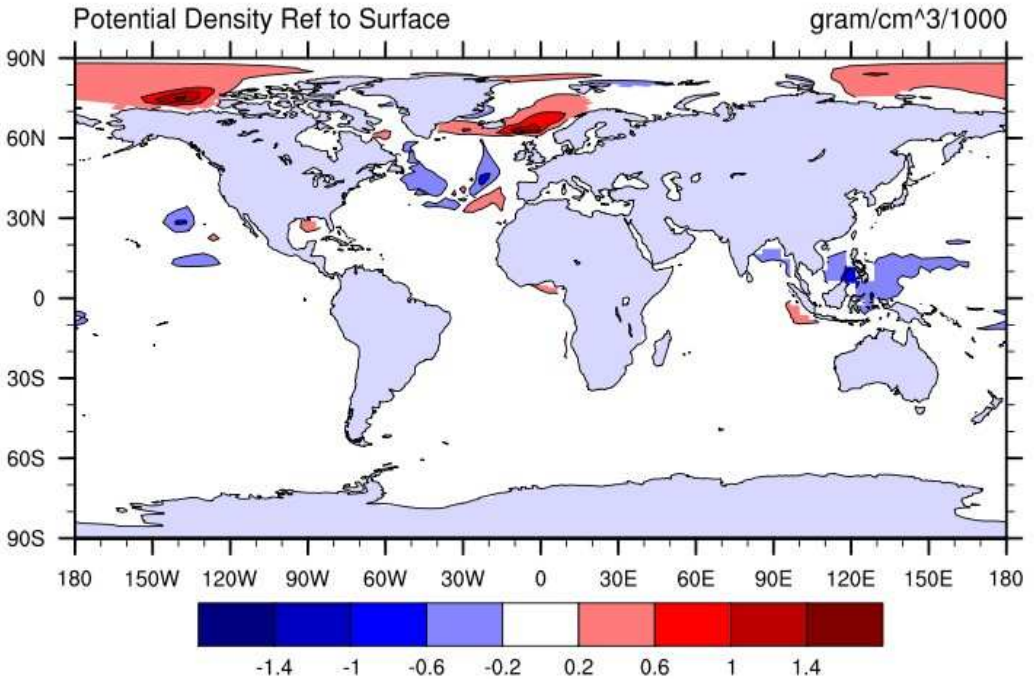

P-E(ACC_B-ACC_A)

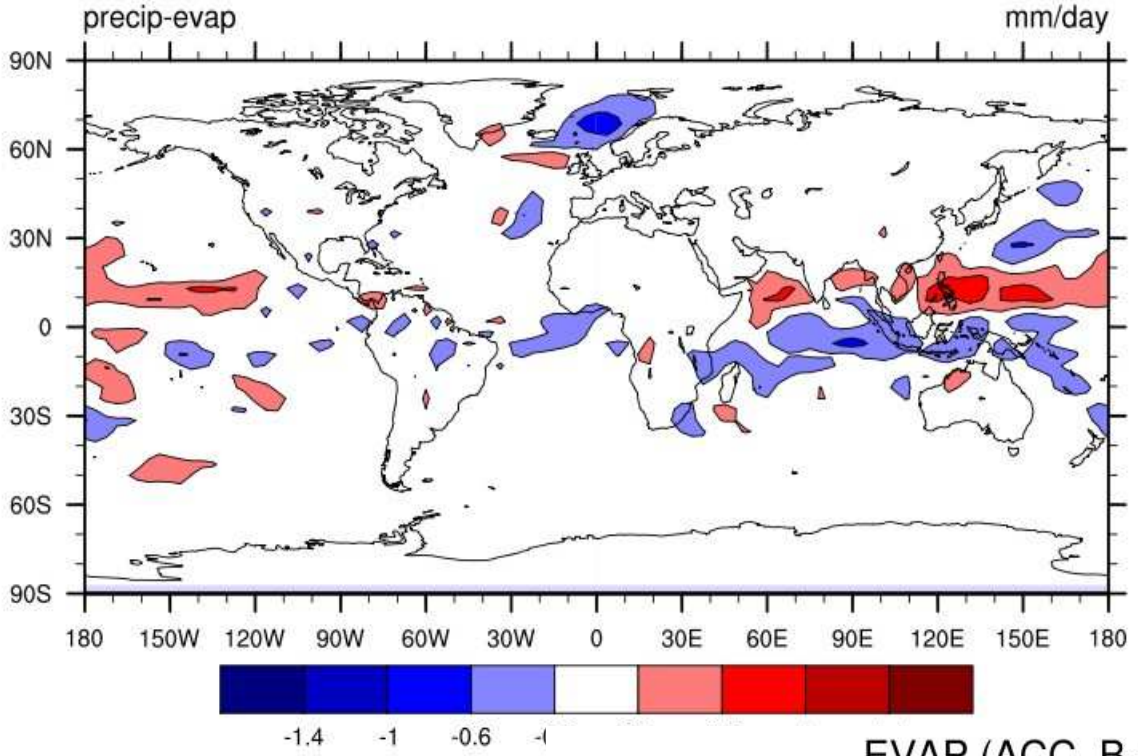

PRECIP (ACC_B-ACC_A)

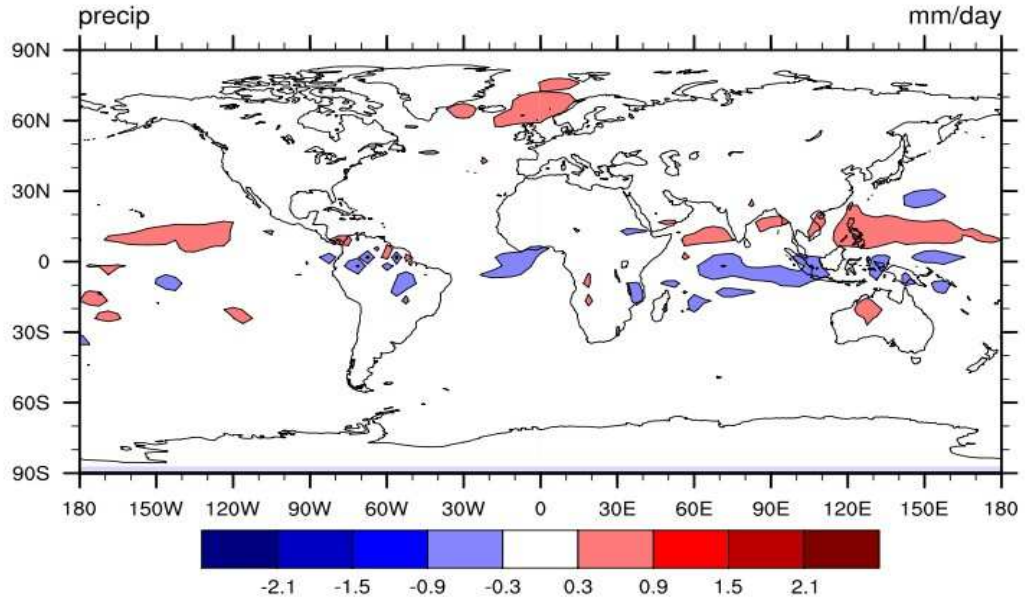

EVAP (ACC_B-ACC_A)

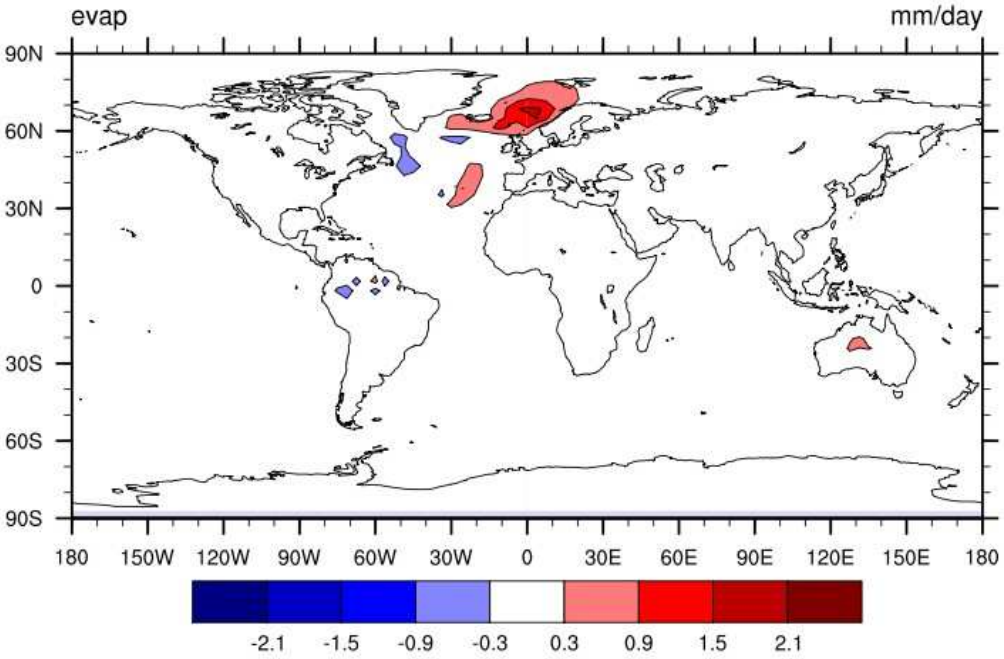

AMOC (ACC_B-ACC_A)

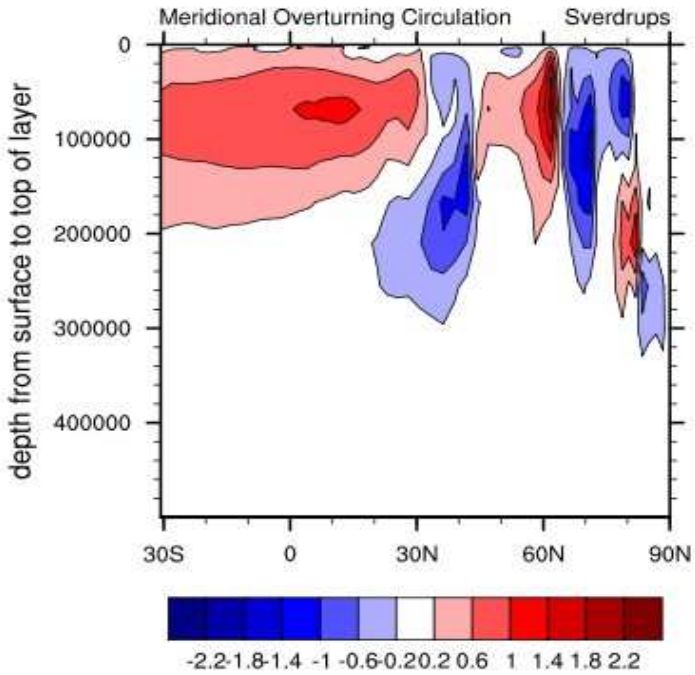

Atlantic Zonal AVG PD (ACC_B-ACC_A)

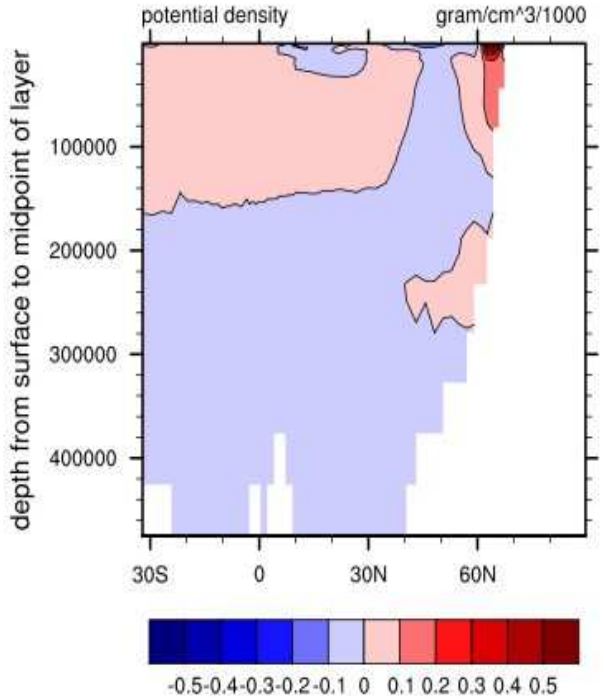

Atlantic Zonal AVG SALT (ACC_B-ACC_A)

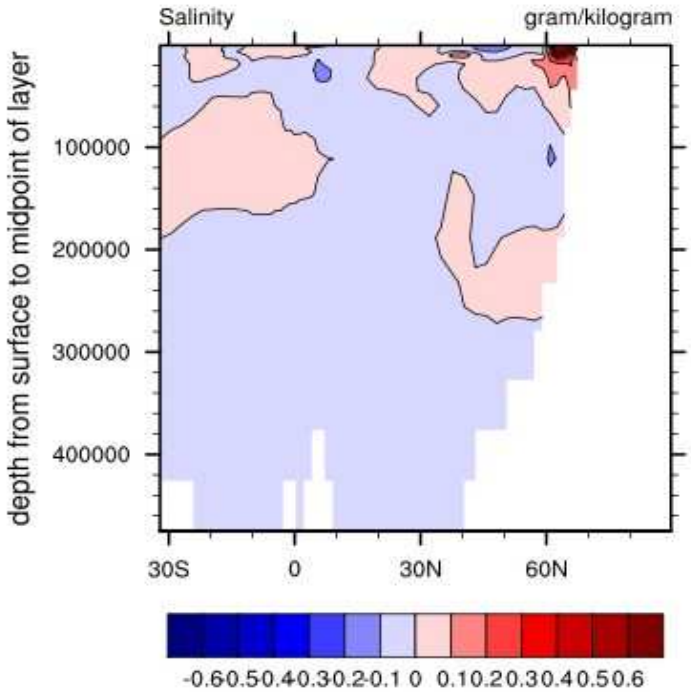

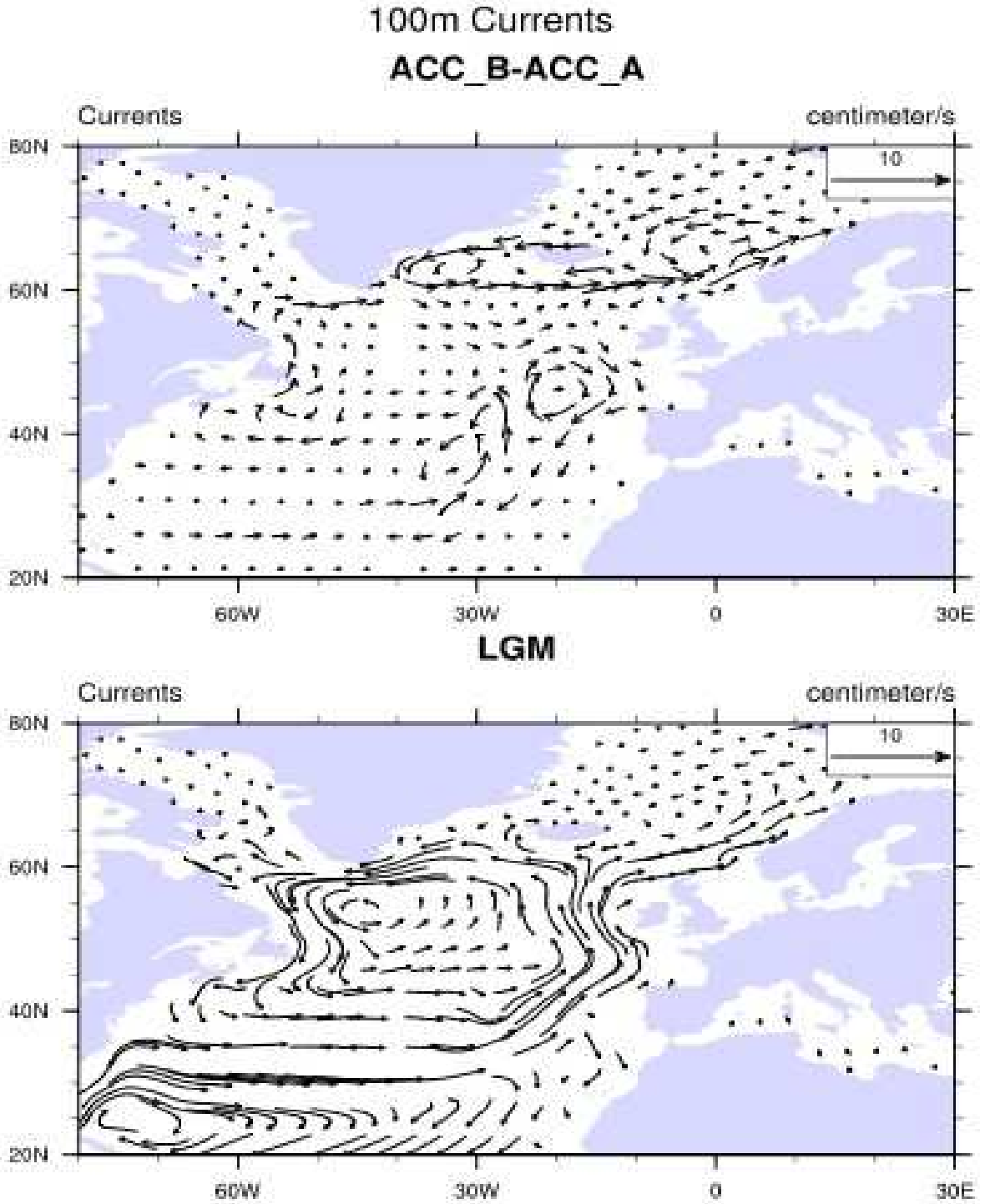
100m Currents
ACC_B-ACC_A
Currents
centimeter/s
10
80N
60N
40N
20N
60W
30W
0
30E
LGM
Currents
centimeter/s
10
80N
60N
40N
20N
60W
30W
0
30E